Hydrogen sulfide bypasses the rate-limiting oxygen activation of heme oxygenase

doi: 10.1074/jbc.RA118.004641

Hydrogen sulfide bypasses the rate-limiting oxygen activation of heme oxygenase

Received for publication, July 9, 2018, and in revised form, August 29, 2018 Published, Papers in Press, September 20, 2018, DOI 10.1074/jbc.RA118.004641

Toshitaka Matsui[‡1], Ryota Sugiyama[‡], Kenta Sakanashi[‡], Yoko Tamura[‡], Masaki Iida[‡], Yukari Nambu[‡], Tsunehiko Higuchi[§], Makoto Suematsu[¶], and Masao Ikeda-Saito[‡2]

From the [‡]Institute of Multidisciplinary Research for Advanced Materials, Tohoku University, Katahira, Aoba, Sendai 980-8577, Japan, [§]Graduate School of Pharmaceutical Sciences, Nagoya City University, Tanabe-dori, Mizuho, Nagoya 467-8603, Japan, and [¶]Department of Biochemistry, Keio University School of Medicine, Shinano-machi, Shinjyuku, Tokyo 160-8582, Japan

Edited by Ruma Banerjee

Discovery of unidentified protein functions is of biological importance because it often provides new paradigms for many research areas. Mammalian heme oxygenase (HO) enzyme catalyzes the O_2-dependent degradation of heme into carbon monoxide (CO), iron, and biliverdin through numerous reaction intermediates. Here, we report that H_2S, a gaseous signaling molecule, is part of a novel reaction pathway that drastically alters HO's products, reaction mechanism, and catalytic properties. Our prediction of this interplay is based on the unique reactivity of H_2S with one of the HO intermediates. We found that in the presence of H_2S, HO produces new linear tetrapyrroles, which we identified as isomers of sulfur-containing biliverdin (SBV), and that only H_2S, but not GSH, cysteine, and polysulfides, induces SBV formation. As BV is converted to bilirubin (BR), SBV is enzymatically reduced to sulfur-containing bilirubin (SBR), which shares similar properties such as antioxidative effects with normal BR. SBR was detected in culture media of mouse macrophages, confirming the existence of this H_2S-induced reaction in mammalian cells. H_2S reacted specifically with a ferric verdoheme intermediate of HO, and verdoheme cleavage proceeded through an O_2-independent hydrolysis-like mechanism. This change in activation mode diminished O_2 dependence of the overall HO activity, circumventing the rate-limiting O_2 activation of HO. We propose that H_2S could largely affect O_2 sensing by mammalian HO, which is supposed to relay hypoxic signals by decreasing CO output to regulate cellular functions. Moreover, the novel H_2S-induced reaction identified here helps sustain HO's heme-degrading and antioxidant-generating capacity under highly hypoxic conditions.

Hydrogen sulfide (H_2S) has emerged as the third gaseous mediator molecule alongside nitric oxide (NO) and carbon monoxide (CO) in mammalian signaling to modulate a variety of biological processes (1–6). H_2S is endogenously synthesized by cystathionine β-synthase (CBS),[3] cystathionine γ-lyase, and 3-mercaptopyruvate sulfurtransferase. Among the gaseous mediators, only H_2S can be ionized in aqueous solution to exist mainly as its monoanion form (SH^-) with negligible amounts of S^{2-} present under physiological pH (pK_a values for H_2S and SH^- are 7.0 and >17, respectively) (6). The SH^- anion is known to possess high reducing ability and nucleophilicity. One of the most established targets of SH^- is a cysteine residue of proteins to form persulfide (–SSH). Functions of target proteins such as ATP-dependent potassium (K_{ATP}) channels (1) are modulated by the covalent modification, which may proceed through nucleophilic attack of SH^- to oxidized forms of the cysteine residue, although the detailed mechanism has yet to be identified (7). In addition, SH^- is reported to react with a variety of small biomolecules to afford reactive sulfur species, including polysulfides (S_n^{2-}) (6, 8, 9). Considering these unique reactivities, H_2S could have further signaling targets, whose identification is crucial for the H_2S biology. We have envisaged a new interplay of H_2S within the gaseous mediator systems because of their tight interactions, especially in vasorelaxation and oxygen (O_2) sensing. For instance, CO binding to a prosthetic heme of CBS inhibits the H_2S synthesis to cause vasoconstriction in neurovascular units (10). The biological source of CO is heme degradation catalyzed by heme oxygenase (HO), which exists as two isoforms, inducible HO-1 and constitutive HO-2 (11). HO activity could have O_2 dependence that is a prerequisite to function as a primary O_2 sensor in the cerebral blood vessels as well as in the carotid body (10, 12). These intricate interplays may be an inherent feature of the gaseous mediators and suggest the existence of further unidentified cross-talk. Here, we report that H_2S opens a novel pathway of HO to produce a new heme catabolite.

The new HO reaction, termed an S-HO reaction hereafter, is predicted on the basis of mechanistic knowledge of HO cataly-

This work was supported by Grants-in-aid for Scientific Research 2412006 and 24350081 (to M. I.-S.); 23550186, 25109504, 15K05555, and 15H00912 (to T. M.); and 17H04000 (to T. H.) from the Japan Society for the Promotion of Science (JSPS) and Ministry of Education, Culture, Sports, Science and Technology (MEXT), Japan; by Takeda Science Foundation; and by Strategic Alliance Project for the Creation of Nano-Materials, and Nano-devices and Nano-systems from MEXT, Japan. The authors declare that they have no conflicts of interest with the contents of this article.
This article was selected as one of our Editors' Picks.
This article contains Figs. S1–S9 and Tables S1 and S2.
[1] To whom correspondence may be addressed. Tel. and Fax: 81-22-217-5117; E-mail: toshitaka.matsui.d5@tohoku.ac.jp.
[2] To whom correspondence may be addressed. Tel. and Fax: 81-22-217-5117; E-mail: mis2@tagen.tohoku.ac.jp.

[3] The abbreviations used are: CBS, cystathionine β-synthase; BV, biliverdin; BR, bilirubin; SBV, sulfur-containing biliverdin; SBR, sulfur-containing bilirubin; HO, heme oxygenase; CPR, cytochrome P450 reductase; BVR, biliverdin reductase; AAPH, 2,2′-azobis(2-amidinopropane) dihydrochloride; ESI, electrospray ionization.

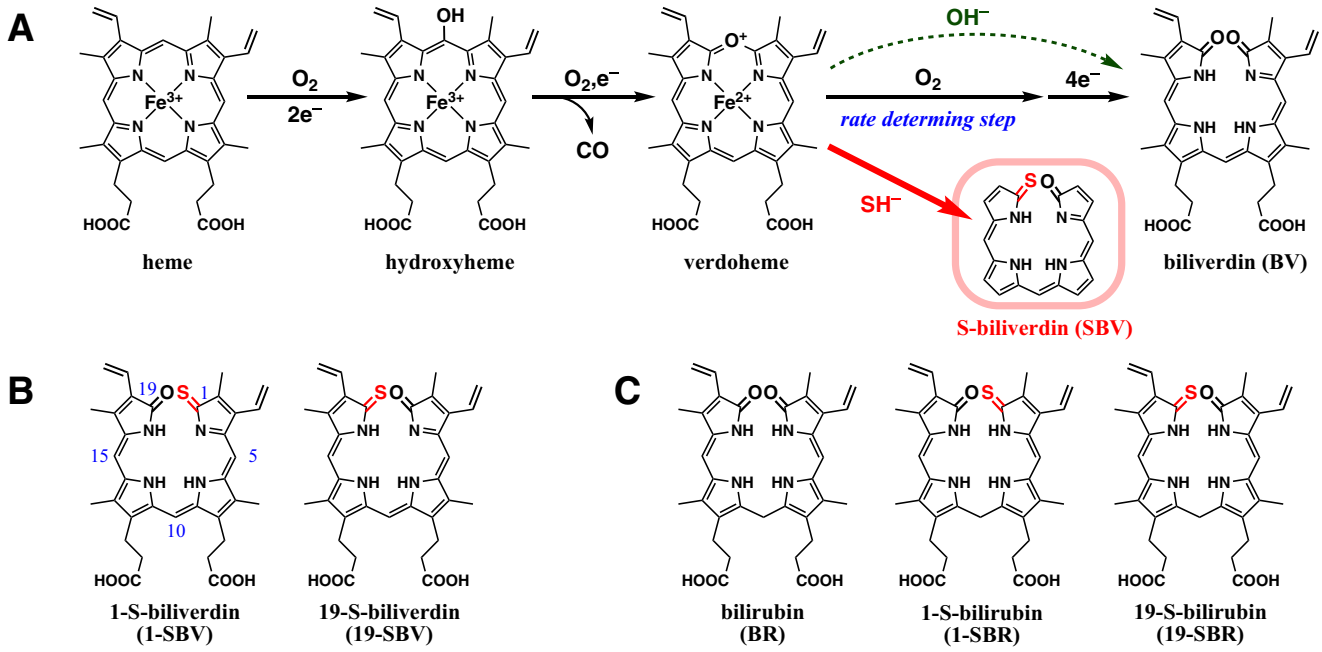

Figure 1. Novel heme degradation induced by H_2S. *A*, initial design of H_2S-induced branching of the HO reaction. Peripheral substituents are omitted for clarity. *B*, structures of SBV isomers. *C*, structures of BR and SBR isomers.

sis as well as H_2S reactivity. HO catalyzes degradation of heme into biliverdin (BV), ferrous iron, and CO by three successive monooxygenation steps via hydroxyheme and verdoheme intermediates (see Fig. 1*A*) (13, 14). These O_2 activation steps are performed by the substrate heme itself, so that HO catalysis actually involves numerous reaction intermediates (Fig. S1) (13, 14). Among them, we have initially postulated the verdoheme intermediate, which may exist in either a ferric or ferrous state (Fig. S1), as a potential target of H_2S. In the enzymatic reaction, the macrocycle of verdoheme is cleaved by reductive O_2 activation on its central iron (15, 16). Anomalously slow O_2 binding on ferrous verdoheme is regarded as a major rate-determining step of HO to achieve the O_2 dependence of its overall activity (15, 17). The other two O_2 reactions with heme and hydroxyheme are not rate-limiting because of their high reactivity and/or affinity (18, 19). Chemically, the verdoheme ring could be cleaved even by O_2-independent hydrolysis (20). Although the verdoheme hydrolysis proceeds only under physiologically irrelevant, strong alkaline conditions, we hypothesized that H_2S efficiently promotes "thiolysis," the hydrolysis-like ring cleavage (see Fig. 1*A*), because of its strong nucleophilicity even under physiological pH. As expected from the reaction design, the S-HO reaction is found to produce an unprecedented sulfur-containing biliverdin termed S-biliverdin (SBV). H_2S reacts with ferric, but not ferrous, verdoheme with drastic modulation of the HO catalytic properties due to circumvention of the rate-limiting O_2 reaction (Fig. 1).

Results

Novel S-HO reaction under single-turnover condition

Effects of H_2S on HO catalysis were first examined under single-turnover conditions where ferric heme complexed with rat HO-1 was converted once into products. In the absence of H_2S, reduction of ferric heme–HO-1 by its physiological redox partner, NADPH-cytochrome P450 reductase (CPR), resulted in an intricate absorption spectral change to eventually afford BV having intense visible absorption around 688 nm (Fig. 2*A*) (21). Temporal emergence of sharp absorption at 641 nm is due to transient accumulation of CO-bound verdoheme (Fig. S1). In the presence of H_2S, the starting heme complex showed a spectral shift typical for partial binding of H_2S to the ferric heme iron (Fig. 2*B*) (22). The heme degradation with H_2S proceeded through distinct intermediate(s) absorbing around 754 nm to yield product(s) having broader absorption at 697 nm. Although H_2S hardly affected amounts of CO produced through the heme degradation (Fig. S4*D*), HPLC analysis detected two new products other than BV in the presence of H_2S (Fig. 2*D*), whose absorption spectra are similar to each other but different from that of BV (Fig. S4*A*). Further product analysis identified these two new products as SBV regioisomers, 1-SBV and 19-SBV (Fig. 1*B*). Positive mass signals of the new products were both found at 599.24 (Fig. S4*C*), consistent with the SBV formula ($[C_{33}H_{34}O_5N_4S + H^+]^+$; calculated *m/z*, 599.23). Isotope labeling experiments revealed incorporation of one each atom of oxygen and sulfur into the new products, whereas BV accepts two oxygen atoms from O_2 at the cleavage site (Table S1). 1-SBV and 19-SBV standards synthesized according to a previous report (23) (Figs. S2 and S3) are indistinguishable from the two new products in terms of the HPLC retention time (Fig. 2*D*) and absorption spectra (Fig. S4, *A* and *B*). These results strongly suggest H_2S-dependent ring cleavage as hypothesized.

Formation and properties of SBR

In mammals, BV is rapidly reduced by biliverdin reductase (BVR) to a yellow pigment, bilirubin (BR; Fig. 1*C* and Fig. S4*E*). The single turnover reaction of the purified HO enzyme with additional BVR yielded BR having typical absorption around

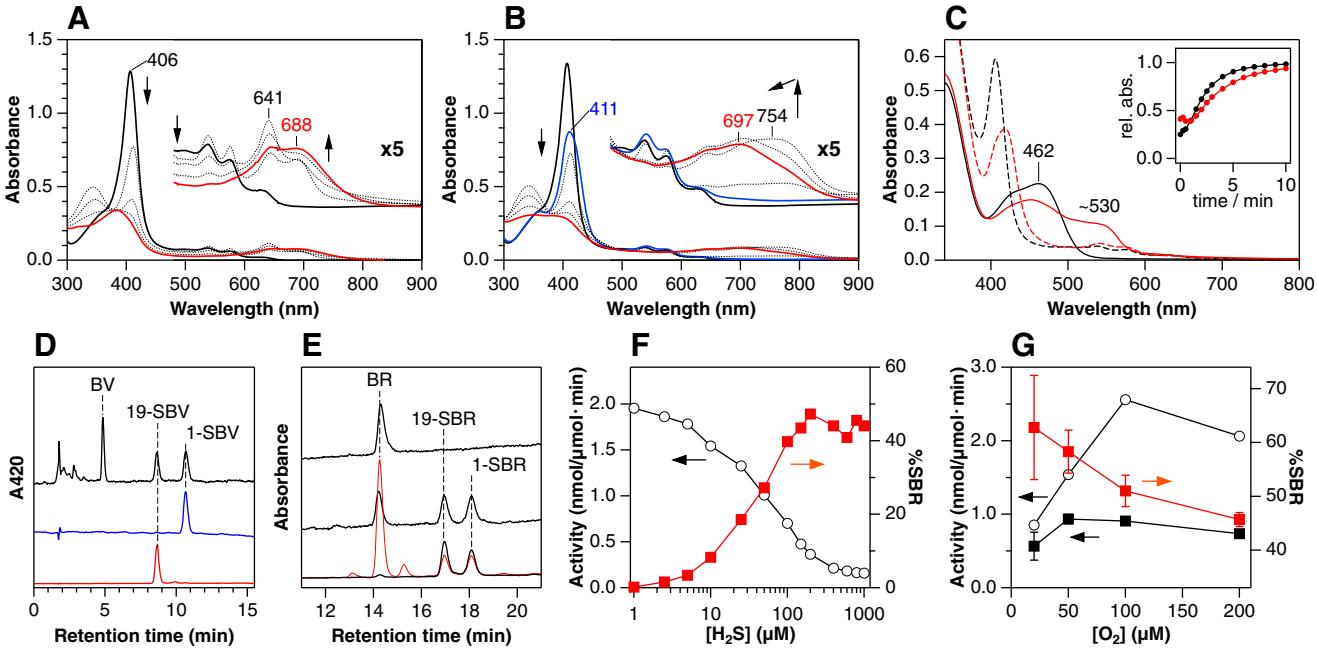

Figure 2. Effects of H_2S on heme degradation by HO. *A* and *B*, absorption spectral changes of heme–HO-1 complexes upon reduction by CPR and NADPH without and with 100 μM H_2S, respectively. Spectra were taken before reaction (*black*) with H_2S (*blue*) and 15 min after addition of CPR (*red*). *C*, spectral changes in the presence of both CPR and BVR before and after reaction of heme–HO-1 (*dashed* and *solid*, respectively) without and with 200 μM H_2S (*black* and *red*, respectively). *Inset*, relative absorbance increase without H_2S at 460 nm (*black*) and with H_2S at 530 nm (*red*). *D*, HPLC chromatograms for the reaction mixture in the presence of H_2S and CPR (*black*) and the 1- and 19-SBV standards (*blue* and *red*, respectively). *E*, HPLC analysis of culture media of RAW264.7 cells treated with hemin (*upper*) and hemin and 2 mM H_2S (*middle*) observed at 520 nm (*black*). *Bottom* traces are chromatograms obtained with mixed standards at 520 (*black*) and 450 nm (*red*). *F*, H_2S dependence of the HO activity (*black*) and the SBR ratio (*red*) under catalytic condition. *G*, O_2 dependence of the catalytic activity (*black squares*) and the SBR ratio (*red squares*) in the presence of 100 μM H_2S of rat HO-1. Catalytic activity was also measured in the absence of H_2S (*open circle*). *Error bars* represent S.E.

462 nm (Fig. 2*C*). The SBV standards were also reduced by BVR to corresponding 1- and 19-SBR isomers (Fig. 1*C*), whose absorption peaks were observed around 530 nm to have distinct orange colors (Fig. S4, *E–G*). Structures of the SBR isomers were further confirmed by various product analyses (Fig. S5, *A–C* and Table S2). Due to the large red shifts of the absorption bands, the SBR formation under the single-turnover condition is easily visualized by an unusual shoulder around 530 nm (Fig. 2*C*). The single turnover rate slightly decreased in the presence of H_2S as judged by absorbance increase either at 460 or 530 nm (approximately half; Fig. 2*C*).

SBR is also produced by a macrophage cell line, RAW264.7. This cell line is reported to secrete BR into cell culture media when incubated with hemin (24). Our HPLC analysis detected only BR as a product of the normal heme catabolism by RAW264.7 (Fig. 2*E*). Addition of H_2S, however, resulted in the formation of the two SBR isomers as well as BR (Fig. 2*E*), assuring the progression of the S-HO reaction in mammalian cells.

The SBR isomers share similar properties with BR as expected from their structural similarity (Fig. 1*C*). Highly hydrophobic SBR and BR require bovine serum albumin (BSA) for their solubilization in neutral buffers. BR is known to be excreted into bile upon glucuronidation in liver (Fig. S5*D*) (25). Both isomers of SBR were similarly converted by UGT1A1 to their mono- and diglucuronides (Fig. S5, *E–G*). BR is also proposed to be a potent antioxidant through a redox cycling with BV (Fig. S6*A*) (26, 27). Catalytic removal of radical species was suggested for BR and the SBR isomers in the 2,2′-azobis(2-amidinopropane) dihydrochloride (AAPH) assay (Fig. S6), implying their comparable potencies as antioxidants.

Catalytic properties of the S-HO reaction

The H_2S effects on HO catalytic properties were examined in the presence of BVR (17). As shown in Fig. 2*F*, the product ratio of total SBR over all three products (%SBR) rose as the H_2S concentration increased (EC_{50} = 34 μM). To our surprise, the catalytic activity of HO-1 was severely suppressed by H_2S (Fig. 2*F*; IC_{50} = 48 μM) despite its small effect on the single turnover rate (Fig. 2*C*). Although the EC_{50} and IC_{50} values are similar at the basal condition ([CPR] = 100 nM), these parameters showed distinct behavior when the CPR concentration was lowered to 20 nM (EC_{50} and IC_{50} = 9.6 and 200 μM, respectively). This observation reveals different mechanisms for the SBR induction and HO inhibition by H_2S. It should also be noted that %SBR was saturated at ~45% under normal air. Incomplete formation of SBR is due, at least in part, to an unexpected action of O_2 because %SBR increased with lowering O_2 concentrations (Fig. 2*G*). O_2 dependence of the catalytic activity was also largely affected by H_2S (Fig. 2*G*). The normal HO reaction without H_2S was slowed down at O_2 concentrations less than 130 μM due to the rate-limiting reaction of the ferrous verdoheme intermediate with O_2 (Fig. 1*A*) (15, 17). In contrast, very little O_2 dependence was observed in the presence of H_2S, consistent with circumvention of the slow O_2-dependent ring cleavage (Fig. 1*A*).

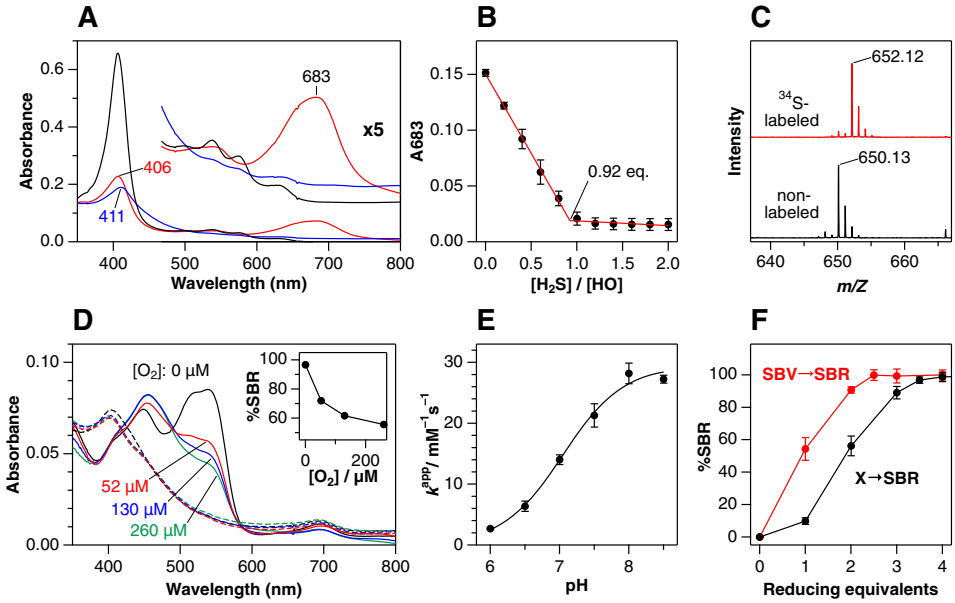

Figure 3. Reactions of ferric verdoheme with H_2S to afford SBR. *A*, spectral changes upon conversion of ferric heme–rat HO-1 (*black*) to ferric verdoheme (*red*) and then to the intermediate X with 100 μM H_2S (*blue*). *B*, titration curve for reaction of ferric verdoheme with H_2S fitted with a piecewise linear function. *C*, ESI-MS spectra (negative ion mode) of the intermediate X prepared with nonlabeled (*black*) and ^{34}S-labeled H_2S (*red*). *D*, absorption spectra of the intermediate X (*dashed*) and its reduced product by CPR and BVR (*solid*) at the indicated O_2 concentrations. *Inset*, SBR ratios determined by HPLC analysis. *E*, pH dependence of apparent rate constants for the reaction between ferric verdoheme and H_2S. *F*, anaerobic titration of X (*black*) and 1-SBV (*red*) with varied amounts of NADPH (2 reducing eq per molecule). SBR formation was estimated from the absorbance increase at 541 nm. *Error bars* represent S.E.

Ferric verdoheme as a branch point intermediate

We finally examined reaction mechanism of the S-HO reaction. In our initial design, H_2S was postulated to attack *ferrous* verdoheme (Fig. 1*A*); however, this intermediate showed negligible spectral change upon addition of H_2S and CPR under anaerobic condition (Fig. S7*A*). Further O_2 addition initiated the reaction but afforded only BR (Fig. S7*A*). Instead, more electrophilic *ferric* verdoheme, which was generated prior to the ferrous form (Fig. S1), was found to rapidly react with H_2S. The H_2S addition to *ferric* verdoheme diminished its characteristic absorption at 683 nm with appearance of featureless, "flat" absorption in a 600–800-nm range (Fig. 3*A*). Resulting intermediate X was reduced to yield a mixture of BR and SBR under normal air, whereas the SBR formation became dominant at lower O_2 concentration (Fig. 3*D*), consistent with the O_2 dependence of %SBR observed in the catalytic assay (Fig. 2*G*). Other HO intermediates generated prior to ferric verdoheme, including hydroxyheme (Fig. S1), did not react with H_2S or only reversibly interacted to eventually afford the same intermediate X (Fig. S7, *B–D*). These results unambiguously identify ferric verdoheme as a branch point intermediate for the BV and SBV pathways of HO as shown in Fig. 4.

Conversion of ferric verdoheme to the intermediate X required approximately 1 molar eq of H_2S (Fig. 3*B*). Mass analysis also revealed incorporation of one sulfur atom into ferric verdoheme (Fig. 3*C* and Fig. S9*A*). Apparent rate constants for the formation of X show pH-dependent transition with a pK_a value of 7.0 (Fig. 3*E*). This change is attributed to ionization of H_2S (pK_a = 7.0) because no significant spectral change was observed for ferric verdoheme in this pH range. The alkaline form (SH^-; 29 mM^{-1} s^{-1}) was ~300-fold more reactive than the acid form (H_2S; 0.094 mM^{-1} s^{-1}), indicating SH^- as a major

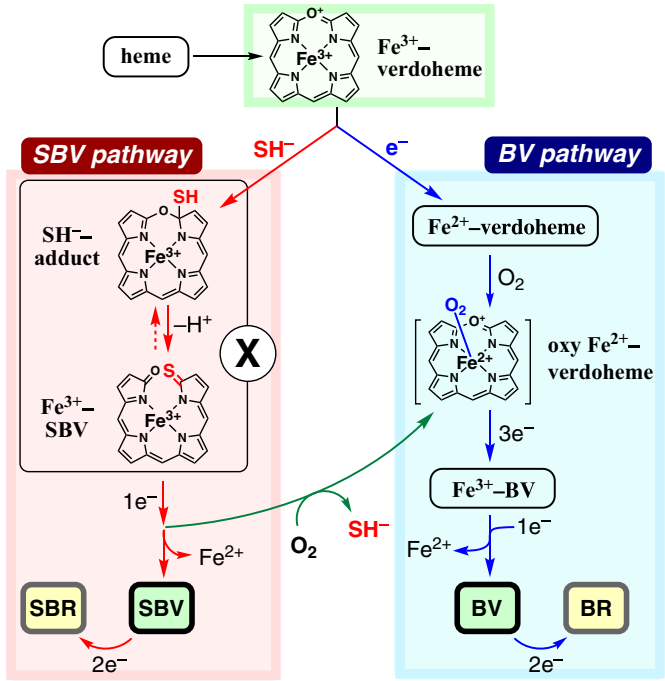

Figure 4. Proposed mechanisms for the heme degradation in the presence of H_2S. Peripheral substituents are omitted for clarity.

reactant. This conclusion rationally explains the low reactivity of other biological thiols. Glutathione (GSH), L-cysteine, and homocysteine, which have higher pK_a values (9.7, 8.4, and 8.9, respectively), showed only limited reactivity with ferric verdoheme (Fig. S8*B*). Moreover, these alkyl thiols did not convert ferric verdoheme to X but reduced it to the ferrous state, leading to the normal BV pathway (Fig. S8*A* and Fig. 4). Similar simple reduction was also observed for sodium polysulfides

(Na_2S_2, Na_2S_3, and Na_2S_4) as shown in Fig. S8, *C* and *D*. Therefore, H_2S is the specific thiol that induces SBV formation.

Ring opening mechanism in the H_2S-mediated reaction

Under anoxic conditions, reduction of the intermediate X dominantly produced SBR (Fig. 3*D*), strongly suggesting an O_2-independent hydrolysis-like mechanism for the SBV production (Fig. 4). In this mechanism, nucleophilic addition of SH^- to a β-pyrrole carbon atom of ferric verdoheme should be followed by deprotonation to cleave the macrocycle. A resulting Fe^{3+}–SBV complex could be reduced by one electron to afford SBV with release of the ferrous iron. As expected from this scheme, the anoxic conversion of X to SBR consumed three electrons, two of which were utilized for reduction of SBV to SBR (Fig. 3*F*). In the presence of O_2, the mechanism became more intricate to afford BV in addition to SBV. The BV formation from X required O_2-induced extrusion of the sulfur atom. X itself has no reactivity with O_2 as judged from the negligible O_2 dependence of its absorption spectra (Fig. 3*D*). Instead, a reduced form of X may bind O_2 on its central iron to liberate the SH^- moiety. This putative reaction yielded oxyferrous verdoheme, which is an intermediate proposed in the normal HO reaction (Fig. 4) (15). The verdoheme regeneration from X is possible because pyridine extraction of X from the protein yielded a bispyridine complex of verdoheme (Fig. S9*B*). It should be also mentioned that one oxygen atom of O_2 was inserted in the conversion of X to BV (Fig. S9*C*), consistent with the O_2 activation on the verdoheme iron (15).

Discussion

In this study, we report the new reaction pathway of mammalian HO induced by H_2S. The gaseous signaling molecule drastically alters the reaction mechanism of HO not only to modulate the catalytic activity and its O_2 dependence but also to produce the new sulfur-containing heme catabolites, 1- and 19-SBV isomers (Fig. 1). It is quite surprising that the classical HO enzyme, whose function and mechanism have been studied in detail over several decades, has an unidentified reaction pathway that is just now being revealed. Recently, noncanonical heme degradation has also been identified for a few bacterial enzymes; however, these enzymes are specifically designed to promote unusual reactions (28–30). We have succeeded in inducing the alternative reaction of the canonical HO enzyme by the rational selection of the small biological molecule to attack its reaction intermediate. H_2S appears to have broad reactivities with many biological compounds. For example, heme is known to interact with H_2S to cause catalytic oxidation of the sulfide (22) and covalent modification of the heme periphery to generate sulfheme (31). These reactions appear to be negligible upon induction of the S-HO reaction (Figs. 2*B* and 3*B*), probably due to the facile and specific reactivity of the HO intermediate with H_2S. Our approach to target the enzyme intermediate thus allows identification of highly specific interactions and could be applied widely to search for hidden functions, especially of well-studied enzymes. Besides the SBV pathway, the HO reaction may branch into unidentified pathways at its numerous reactive intermediates (Fig. S1) by choosing other appropriate small molecules. Moreover, H_2S could react with enzymes other than HO to bring out their unidentified reactions. To discover further unknown targets, possible effects of H_2S should be extensively studied for reactions involving hydrolysis or a step replaceable with a hydrolysis-type reaction in addition to searching for electrophilic intermediates.

We have almost fully elucidated the formation mechanism of SBV. The SH^- ion binds to ferric verdoheme and cleaves the macrocycle in an O_2-independent manner. The only major ambiguity remaining is the nature of the observed intermediate X. The intermediate X generated in the reaction between ferric verdoheme and H_2S can be either an SH^-–adduct of verdoheme or an Fe^{3+}–SBV complex (Fig. 4), both of which match the mass data (Fig. 3*C* and Fig. S9*A*). The SH^-–adduct form well explains the O_2-dependent SH^- extrusion, whereas ring closure of Fe^{3+}–SBV seems not to occur easily. Nevertheless, the absorption spectrum of X, especially its flat absorption in the visible region, is very similar to that of the Fe^{3+}–BV complex (Fig. 3*A* and Fig. S9*D*) (32), strongly suggesting the Fe^{3+}–SBV structure for X. The ring closure may proceed more easily than we expected to achieve equilibrium of the open and closed ring structures for X and/or its reduced form.

Successful detection of SBR assures that the S-HO reaction can take place in mammalian cells (Fig. 2*E*). Nevertheless, we cannot specify the H_2S concentration required for the SBV induction (EC_{50}) *in vivo*. Our mechanistic analysis identifies ferric verdoheme as a branch point intermediate for the normal and SBV pathways (Fig. 4). Because the SH^- addition and reduction of ferric verdoheme are essentially irreversible, a major determinant of the EC_{50} value should be relative rates of the two competing reactions. Slower reduction by CPR hence results in the lowered EC_{50} value as shown for the *in vitro* assay. Some naturally occurring mutations of CPR are known to significantly suppress electron transfer to HO (33), probably leading to hypersensitivity toward H_2S. Hypoxia is also expected to decelerate the electron transfer by inducing liberation of HO from the endoplasmic reticulum (34). The cytosolic HO enzyme could interact only weakly with CPR remaining on the endoplasmic reticulum membrane. The SBV formation could be enhanced under hypoxia because of the slow reduction as well as the low O_2 concentration. Nonmammalian HOs with greater diversity in structure and reactivity may have larger deviations in the H_2S requirement to stimulate the S-HO reaction. Even non-HO–type heme-degrading enzymes involving ferric verdoheme in their catalysis are possible targets of H_2S (35). Our finding clearly indicates the necessity to take the possible interplay between H_2S and heme degradation into account in all related research areas.

The new S-HO reaction could have large impacts on physiological functions of H_2S and HO through drastic changes in both the product and catalytic activity of HO. Properties of the new heme catabolites have been examined mainly for their reduced form, SBR, which as well as BR should be the major form in mammalian cells. Although BR is crucial in mammals as a causative agent of jaundice and a potent antioxidant (26), SBR shows solubility, glucuronidation potency, and redox properties similar to those of BR (Figs. S5, *D–G*, and S6). This observation implies that H_2S does not greatly alter antioxidative

functions of the HO reaction in mammals. Biological roles of SBV are yet to be examined, especially in biosynthesis of phytochromes and photoreceptor proteins in plants, bacteria, and fungi, which utilize BV or its derivatives as a pigment for detecting red and far-red light (36).

Our catalytic assay reveals the O_2-dependent change of the SBR production ratio (%SBR) due to the O_2-induced return to the BV pathway (Figs. 2*G* and 4). Considering the similar properties of BR and SBR, this product change itself may have a biological significance only when a receptor system specific to the new catabolite exists. More importantly, the O_2 dependence of the HO activity was lost in the presence of H_2S due to circumvention of the rate-limiting O_2 activation by ferrous verdoheme (Figs. 2*G* and 4) (10, 15, 37). This activity change is expected to have large impacts on gas signaling, namely the O_2 sensing in the brain microvessels as well in as the carotid body. In these systems, HO-2, a constitutive isoform of HO, serves as a primary oxygen sensor, and its CO product is considered to transduce the O_2 signal in concert with H_2S (10, 12, 38). A major H_2S generator in brain is CBS (39), whose prosthetic heme group binds CO to directly inhibit the enzyme activity under normoxia (40). CO is also reported to be a physiological inhibitor of cystathionine γ-lyase in the carotid body despite the absence of an apparent CO-binding site (41). Under hypoxic condition, the HO activity decreases to relieve the CO inhibition of the H_2S-generating enzymes. Consequently, hypoxia stimulates the H_2S synthesis to enhance vasodilation in brain and neural activity of the carotid body through regulation of potassium channels (10, 38). The faster formation of H_2S together with its slower decay through O_2-dependent processes is expected to promote the O_2-independent S-HO reaction under hypoxia (Figs. 2*G* and 4). This maintains the HO activity at a certain level even under highly hypoxic conditions to avoid a complete stop of CO synthesis and thus overproduction of H_2S. An H_2S concentration ceiling may be important to prevent respiratory disorder (42) and to reduce its toxicity. Likewise, under inflammatory conditions in which cytokines activate macrophages, the cells induce HO-1 (43), which might protect against oxidative stress through the action of SBV and SBR under hypoxic conditions.

Another striking effect of H_2S is severe suppression of the HO catalytic activity (Fig. 2*F*), which is not explained by the mechanism shown in Fig. 4. Considering the weak inhibition of the single turnover reaction (Fig. 2*C*), interference by H_2S appears to occur at a step prior to formation of the heme–HO complex. Under the catalytic conditions, excess hemin weakly binds to BSA supplemented to solubilize the BR and SBR products. The hemin–BSA complex exhibits a significant spectral change when incubated with H_2S under hypoxic conditions but not under air, suggesting temporal reduction of hemin, O_2 binding, and rapid auto-oxidation. This implies catalytic production of reactive oxygen species, which may inactivate the HO enzyme. The inhibitory effect of H_2S *in vivo* might be distinct from our *in vitro* observation because it would largely depend on the status of "free heme" that interacts with various cellular factor(s).

Experimental procedures

Materials

$^{18}O_2$ and $^{34}S_8$ were purchased from Spectra Stable Isotope (^{18}O content, >95%) and ISOFLEX (^{34}S content, 99.9%), respectively. Liquid NH_3 (20 ml) was added dropwise to $^{34}S_8$ (100 mg, 2.94 mmol) and sodium (135 mg, 5.89 mmol) in a round-bottom flask at −78 °C. The reaction mixture was stirred at room temperature under an argon atmosphere until liquid NH_3 entirely vaporized. The residue was dried under reduced pressure to afford $Na_2{}^{34}S$ (anhydrous) as pale yellow powder (233 mg, quantitative). Microsomes containing human UGT1A1 and reagents required for glucuronidation were obtained from BD Gentest. Preparation of rat HO-1, its hemin complex, human CPR, and BVR was carried out as described previously (44–46). Other chemicals and proteins were obtained from Wako, Oriental Yeast, Sigma-Aldrich, or ICN and used without further purification. RAW264.7 was purchased from the American Type Culture Collection (ATCC). The basal buffer used throughout this study was 0.1 M HEPES, pH 7.5, at 20 °C unless otherwise stated.

Heme degradation by purified enzyme systems

Single turnover reactions to yield BV/SBV were typically examined in the presence of 10 μM ferric heme–HO-1, 40 μM NADPH, 40 nM CPR, and varied amounts of H_2S. Similar single turnover reactions for BR/SBR were supplemented further with 40 nM BVR and 10 μM BSA. Catalytic assays were conducted with 0.25 μM HO-1, 10 μM hemin, 200 μM NADPH, 100 nM CPR, 25 nM BVR, 15 μM BSA, 100 units/ml catalase, 10 units/ml superoxide dismutase, and varied concentrations of H_2S. Initial rates were determined at 20 min to assure linear increase of the products. O_2 dependence of the catalytic activity and $^{18}O_2$ labeling of the products were examined in an anaerobic glove box (UNIlab, MBraun). Absorption spectral changes during the reaction were recorded by an Agilent 8453 or Shimadzu UV-1500 spectrophotometer.

Product analysis of enzymatic reactions

Heme catabolites were concentrated by solid-phase extraction with Supelclean LC-18 columns (Supelco) as described elsewhere (15). The BR/SBR extraction was operated under minimum light to suppress their photoisomerization. Benzophenone was added as an internal standard at the end of the reactions for quantitative experiments. HPLC analyses of the extracted products were performed on a Shimadzu LC-20 HPLC system equipped with an SPD-M20A photodiode array detector at a flow rate of 1.0 ml/min. The BV/SBV products were separated on a Tosoh ODS-80Ts reversed-phase column (4.6 × 150 mm) with an isocratic elution of 70% methanol and 30% 0.1 M ammonium acetate (v/v). The BR/SBR analysis was performed typically on the ODS-80Ts column with a linear gradient from 75% methanol, 25% 20 mM triethylamine, and acetic acid (v/v), pH 5.0, to 85% methanol (v/v) over 15 min.

ESI-MS spectra were measured on a Bruker micrOTOF-Q-II mass spectrometer equipped with an Agilent 1100 HPLC system at a flow rate of 0.2 ml/min. LC separation of BV/SBV was conducted on the ODS-80Ts column (2.0 × 150 mm) with an

isocratic elution of 20% 0.1 M ammonium acetate and 80% methanol (v/v). BR/SBR and their glucuronides were analyzed with an Agilent ZORBAX Extend-C18 reversed-phase column (2.1 × 150 mm) using a linear gradient from 35% methanol and 65% 20 mM aqueous ammonia (v/v) to 50% methanol (v/v) over 20 min. Mass spectra of the intermediate X were measured by direct infusion at 3 μl/min of a reaction solution containing 3 μM heme–HO-1, 10 μM H_2O_2, and 20 μM H_2S. Typical parameters for the MS measurements were as follows: end plate offset, −500 V; capillary, 4500 V; in-source collision-induced dissociation, 150 V; nebulizer gas, 0.4 bar; dry gas, 4.0 liters/min; dry gas temperature, 180 °C.

CO was quantitated using an H64L variant of myoglobin having high CO affinity as reported earlier (28). After completion of single turnover reactions of 4 μM heme–HO-1, solid sodium dithionite and then H64L myoglobin (final concentration, 6 μM) were added to record absorption spectra of H64L partially bound with CO. Subtraction of a spectrum of ferrous H64L without exogenous ligands generated difference spectra in which a positive peak indicates generation of the CO-bound form and a negative peak is due to disappearance of ferrous deoxy H64L.

Synthesis of 1- and 19-SBV

1- and 19-SBV isomers were synthesized as their dimethyl esters (total yields from BV, 22 and 15%, respectively) according to a previous report (23). ^1H and ^{13}C NMR of the dimethyl esters was measured in $CDCl_3$ with JEOL JMN-LA400 and JMN-LA600 Fourier transform NMR spectrometers (Figs. S2 and S3). Chemical shifts were referenced internally to $CDCl_3$. The SBV esters were hydrolyzed, purified, and weighed by a Sartorius ultra-microbalance SE2 to determine extinction coefficients (Fig. S4, *F* and *G*).

Glucuronidation

Approximately 20 μM SBV isomers were reduced by BVR to corresponding SBR isomers in the presence of 20 μM NADPH and 30 μM BSA. The freshly prepared SBR was glucuronidated at 37 °C by BD Supersomes UGT1A1 according to a protocol provided by the manufacturer. Aliquots of samples were analyzed by HPLC and ESI-MS.

AAPH assay

Each of 10 μM freshly prepared BR and SBR isomers was incubated at 37 °C with 50 mM AAPH in 0.1 M potassium phosphate, pH 7.5, containing 200 mM NaCl and 15 μM BSA with or without 100 μM NADPH and 50 nM BVR. Absorption spectral changes during the reaction were monitored at 468, 541, and 521 nm for BR, 1-SBR, and 19-SBR, respectively.

Heme degradation by mammalian cells

RAW264.7 cells were maintained in a 37 °C humidified incubator containing 5% CO_2 and cultured in Dulbecco's modified Eagle's medium supplemented with 10% fetal bovine serum, penicillin-streptomycin, and glutamine. 9×10^6 cells were grown in a 75-cm^2 cell culture flask for 24 h and then incubated with 20 μM hemin for 12 h to induce HO-1. For efficient removal of BR generated during the induction period, the cells and the flask were washed three times with the culture medium containing fetal bovine serum rather than PBS. Heme degradation was performed by incubating the cells in fresh medium (18 ml) containing 5 μM hemin and 2 mM H_2S at 37 °C. The screw cap of the flask was closed during the reaction to suppress volatilization of H_2S. The medium was recovered after 2-h incubation, centrifuged (3,000 rpm for 5 min), and supplemented with propiophenone as an internal standard. Further addition of a half-volume of saturated guanidine hydrochloride was followed by solid-phase extraction and HPLC analysis as noted above.

Preparation of HO intermediates

Ferric heme–HO-1 as purified was reduced by a slight excess of dithionite anaerobically in the glove box to afford ferrous deoxyheme–HO-1 to which 100 μl of air was bubbled to yield ferrous oxyheme–HO-1. Ferric hydroxyheme–HO-1 was generated in an anaerobic reaction of ferric heme–HO-1 with a slight excess of H_2O_2 (47). Reaction of ferric heme–HO-1 with H_2O_2 under air yields ferric verdoheme–HO-1 (48). Alternatively, ferric verdoheme–HO-1 was generated upon oxidation of ferrous verdoheme–HO-1, which was prepared as described earlier (15), by 3 molar eq of potassium ferricyanide ($K_3[Fe(CN)_6]$). The latter method enables completely anoxic preparation of ferric verdoheme. Ferric biliverdin–HO-1 was prepared from ferric heme–HO-1 by ascorbate-dependent heme degradation.

Reaction of ferric verdoheme–HO-1 with H_2S

The ferric verdoheme complex was prepared by H_2O_2 immediately prior to use and used within 5 min after adding catalase to remove the residual peroxide. Reactions with alkyl thiols were performed in the presence of CO to suppress auto-oxidation of ferrous verdoheme. Kinetic analysis of ferric verdoheme–HO-1 with H_2S was performed at 20 °C using a UNISOKU RSP-601 stopped-flow apparatus equipped with a built-in rapid scan spectrophotometer. The ferric verdoheme complex (3 μM) was mixed with equal volumes of H_2S solution (final concentration, 50–200 μM). Observed rate constants determined from absorbance change at 683 nm exhibited good linear relationships with the H_2S concentrations to afford apparent reaction rate constants (k_{app}) at varied pH. pH dependence of the k_{app} values (Fig. 3*E*) is well-fitted by assuming an acid-base transition of H_2S (pK_a 7.0). Buffers used for the kinetic analysis were: 0.1 M citrate, pH 6.0–7.0; phosphate, pH 6.5–7.5; HEPES, pH 7.0–8.0; and Tris-HCl, pH 7.5–8.5.

Product formation from X

The intermediate X was prepared anaerobically from ferrous verdoheme as noted above. The reductive titration to SBR was performed under anoxic condition while monitoring absorbance increase at 541 nm. Formal two-electron reduction of SBV to SBR was confirmed for the stable 1-SBV isomer. To examine O_2 dependence of the product distribution, the anoxic X was mixed with air-saturated buffer to fill the screw-top cuvette. Products were quantitated by HPLC analysis. For isotope labeling of BV generated through O_2-dependent reaction of X, the intermediate was prepared with a slight excess of non-

labeled H_2O_2 and air, which was followed by addition of catalase and bubbling with excess $^{18}O_2$.

Author contributions—T. M., M. S., and M. I.-S. conceptualization; T. M. and M. I.-S. funding acquisition; T. M., R. S., K. S., Y. T., M. I., Y. N., and T. H. investigation; T. M. and M. I.-S. writing-original draft; T. M. and M. I.-S. project administration; M. S. and M. I.-S. writing-review and editing.

Acknowledgments—A portion of this work was supported by metabolomics platform established by JST, ERATO, Suematsu Gas Biology (completed in March 2015). We thank Drs. C. S. Raman, Emma Raven, and Sofia M. Kapetanaki for their helpful comments.

References

1. Paul, B. D., and Snyder, S. H. (2012) H_2S signalling through protein sulfhydration and beyond. *Nat. Rev. Mol. Cell Biol.* **13,** 499–507 CrossRef Medline
2. Kimura, H. (2011) Hydrogen sulfide: its production, release and functions. *Amino Acids* **41,** 113–121 CrossRef Medline
3. Kajimura, M., Fukuda, R., Bateman, R. M., Yamamoto, T., and Suematsu, M. (2010) Interactions of multiple gas-transducing systems: hallmarks and uncertainties of CO, NO, and H_2S gas biology. *Antioxid. Redox Signal.* **13,** 157–192 CrossRef Medline
4. Suematsu, M., Goda, N., Sano, T., Kashiwagi, S., Egawa, T., Shinoda, Y., and Ishimura, Y. (1995) Carbon monoxide: an endogenous modulator of sinusoidal tone in the perfused rat liver. *J. Clin. Investig.* **96,** 2431–2437 CrossRef Medline
5. Kabe, Y., Nakane, T., Koike, I., Yamamoto, T., Sugiura, Y., Harada, E., Sugase, K., Shimamura, T., Ohmura, M., Muraoka, K., Yamamoto, A., Uchida, T., Iwata, S., Yamaguchi, Y., Krayukhina, E., *et al.* (2016) Haem-dependent dimerization of PGRMC1/Sigma-2 receptor facilitates cancer proliferation and chemoresistance. *Nat. Commun.* **7,** 11030 CrossRef Medline
6. Filipovic, M. R., Zivanovic, J., Alvarez, B., and Banerjee, R. (2018) Chemical biology of H_2S signaling through persulfidation. *Chem. Rev.* **118,** 1253–1337 CrossRef Medline
7. Mishanina, T. V., Libiad, M., and Banerjee, R. (2015) Biogenesis of reactive sulfur species for signaling by hydrogen sulfide oxidation pathways. *Nat. Chem. Biol.* **11,** 457–464 CrossRef Medline
8. Nishida, M., Sawa, T., Kitajima, N., Ono, K., Inoue, H., Ihara, H., Motohashi, H., Yamamoto, M., Suematsu, M., Kurose, H., van der Vliet, A., Freeman, B. A., Shibata, T., Uchida, K., Kumagai, Y., *et al.* (2012) Hydrogen sulfide anion regulates redox signaling via electrophile sulfhydration. *Nat. Chem. Biol.* **8,** 714–724 CrossRef Medline
9. Shiota, M., Naya, M., Yamamoto, T., Hishiki, T., Tani, T., Takahashi, H., Kubo, A., Koike, D., Itoh, M., Ohmura, M., Kabe, Y., Sugiura, Y., Hiraoka, N., Morikawa, T., Takubo, K., *et al.* (2018) Gold-nanofève surface-enhanced Raman spectroscopy visualizes hypotaurine as a robust anti-oxidant consumed in cancer survival. *Nat. Commun.* **9,** 1561 CrossRef Medline
10. Morikawa, T., Kajimura, M., Nakamura, T., Hishiki, T., Nakanishi, T., Yukutake, Y., Nagahata, Y., Ishikawa, M., Hattori, K., Takenouchi, T., Takahashi, T., Ishii, I., Matsubara, K., Kabe, Y., Uchiyama, S., *et al.* (2012) Hypoxic regulation of the cerebral microcirculation is mediated by a carbon monoxide-sensitive hydrogen sulfide pathway. *Proc. Natl. Acad. Sci. U.S.A.* **109,** 1293–1298 CrossRef Medline
11. Maines, M. D. (1997) The heme oxygenase system: a regulator of second messenger gases. *Annu. Rev. Pharmacol. Toxicol.* **37,** 517–554 CrossRef Medline
12. Williams, S. E., Wootton, P., Mason, H. S., Bould, J., Iles, D. E., Riccardi, D., Peers, C., and Kemp, P. J. (2004) Hemoxygenase-2 is an oxygen sensor for a calcium-sensitive potassium channel. *Science* **306,** 2093–2097 CrossRef Medline
13. Matsui, T., Unno, M., and Ikeda-Saito, M. (2010) Heme oxygenase reveals its strategy for catalyzing three successive oxygenation reactions. *Acc. Chem. Res.* **43,** 240–247 CrossRef Medline
14. Montellano, P. R. (2000) The mechanism of heme oxygenase. *Curr. Opin. Chem. Biol.* **4,** 221–227 CrossRef Medline
15. Matsui, T., Nakajima, A., Fujii, H., Matera, K. M., Migita, C. T., Yoshida, T., and Ikeda-Saito, M. (2005) O_2- and H_2O_2-dependent verdoheme degradation by heme oxygenase: Reaction mechanisms and potential physiological roles of the dual pathway degradation. *J. Biol. Chem.* **280,** 36833–36840 CrossRef Medline
16. Matsui, T., Omori, K., Jin, H., and Ikeda-Saito, M. (2008) Alkyl peroxides reveal the ring opening mechanism of verdoheme catalyzed by heme oxygenase. *J. Am. Chem. Soc.* **130,** 4220–4221 CrossRef Medline
17. Liu, Y., and Ortiz de Montellano, P. R. (2000) Reaction intermediates and single turnover rate constants for the oxidation of heme by human heme oxygenase-1. *J. Biol. Chem.* **275,** 5297–5307 CrossRef Medline
18. Migita, C. T., Matera, K. M., Ikeda-Saito, M., Olson, J. S., Fujii, H., Yoshimura, T., Zhou, H., and Yoshida, T. (1998) The oxygen and carbon monoxide reactions of heme oxygenase. *J. Biol. Chem.* **273,** 945–949 CrossRef Medline
19. Matera, K. M., Takahashi, S., Fujii, H., Zhou, H., Ishikawa, K., Yoshimura, T., Rousseau, D. L., Yoshida, T., and Ikeda-Saito, M. (1996) Oxygen and one reducing equivalent are both required for the conversion of α-hydroxyhemin to verdoheme in heme oxygenase. *J. Biol. Chem.* **271,** 6618–6624 CrossRef Medline
20. Saito, S., and Itano, H. A. (1982) Verdohemochrome IXα: preparation and oxidoreductive cleavage to biliverdin IXα. *Proc. Natl. Acad. Sci. U.S.A.* **79,** 1393–1397 CrossRef Medline
21. Matsui, T., Furukawa, M., Unno, M., Tomita, T., and Ikeda-Saito, M. (2005) Roles of distal Asp in heme oxygenase from *Corynebacterium diphtheriae*, HmuO: a water-driven oxygen activation mechanism. *J. Biol. Chem.* **280,** 2981–2989 CrossRef Medline
22. Bostelaar, T., Vitvitsky, V., Kumutima, J., Lewis, B. E., Yadav, P. K., Brunold, T. C., Filipovic, M., Lehnert, N., Stemmler, T. L., and Banerjee, R. (2016) Hydrogen sulfide oxidation by myoglobin. *J. Am. Chem. Soc.* **138,** 8476–8488 CrossRef Medline
23. Fuhrhop, J. H., and Kruger, P. (1977) 1- or 19-methoxy-, 1- or 19-amino- and 1- or 19-thio-deoxybiliverdins. *Liebigs Ann. Chem.* **1977,** 360–370 CrossRef
24. Park, J. H., Oh, S. M., Lim, S. S., Lee, Y. S., Shin, H. K., Oh, Y. S., Choe, N. H., Park, J. H., and Kim, J. K. (2006) Induction of heme oxygenase-1 mediates the anti-inflammatory effects of the ethanol extract of *Rubus coreanus* in murine macrophages. *Biochem. Biophys. Res. Commun.* **351,** 146–152 CrossRef Medline
25. Bosma, P. J., Seppen, J., Goldhoorn, B., Bakker, C., Oude Elferink, R. P., Chowdhury, J. R., Chowdhury, N. R., and Jansen, P. L. (1994) Bilirubin UDP-glucuronosyltransferase 1 is the only relevant bilirubin glucuronidating isoform in man. *J. Biol. Chem.* **269,** 17960–17964 Medline
26. Baranano, D. E., Rao, M., Ferris, C. D., and Snyder, S. H. (2002) Biliverdin reductase: a major physiologic cytoprotectant. *Proc. Natl. Acad. Sci. U.S.A.* **99,** 16093–16098 CrossRef Medline
27. Stocker, R., Yamamoto, Y., McDonagh, A. F., Glazer, A. N., and Ames, B. N. (1987) Bilirubin is an antioxidant of possible physiological importance. *Science* **235,** 1043–1046 CrossRef Medline
28. Nambu, S., Matsui, T., Goulding, C. W., Takahashi, S., and Ikeda-Saito, M. (2013) A new way to degrade heme: the *Mycobacterium tuberculosis* enzyme MhuD catalyzes heme degradation without generating CO. *J. Biol. Chem.* **288,** 10101–10109 CrossRef Medline
29. Matsui, T., Nambu, S., Goulding, C. W., Takahashi, S., Fujii, H., and Ikeda-Saito, M. (2016) Unique coupling of mono- and dioxygenase chemistries in a single active site promotes heme degradation. *Proc. Natl. Acad. Sci. U.S.A.* **113,** 3779–3784 CrossRef Medline
30. LaMattina, J. W., Nix, D. B., and Lanzilotta, W. N. (2016) Radical new paradigm for heme degradation in *Escherichia coli* O157:H7. *Proc. Natl. Acad. Sci. U.S.A.* **113,** 12138–12143 CrossRef Medline
31. Johnson, E. A. (1970) The reversion to haemoglobin of sulphhaemoglobin and its coordination derivatives. *Biochim. Biophys. Acta* **207,** 30–40 CrossRef Medline

32. Yoshida, T., and Kikuchi, G. (1978) Features of the reaction of heme degradation catalyzed by the reconstituted microsomal heme oxygenase system. *J. Biol. Chem.* **253,** 4230–4236 Medline
33. Marohnic, C. C., Huber Iii, W. J., Patrick Connick, J., Reed, J. R., McCammon, K., Panda, S. P., Martásek, P., Backes, W. L., and Masters, B. S. (2011) Mutations of human cytochrome P450 reductase differentially modulate heme oxygenase-1 activity and oligomerization. *Arch. Biochem. Biophys.* **513,** 42–50 CrossRef Medline
34. Lin, Q., Weis, S., Yang, G., Weng, Y. H., Helston, R., Rish, K., Smith, A., Bordner, J., Polte, T., Gaunitz, F., and Dennery, P. A. (2007) Heme oxygenase-1 protein localizes to the nucleus and activates transcription factors important in oxidative stress. *J. Biol. Chem.* **282,** 20621–20633 CrossRef Medline
35. Uchida, T., Sekine, Y., Dojun, N., Lewis-Ballester, A., Ishigami, I., Matsui, T., Yeh, S. R., and Ishimori, K. (2017) Reaction intermediates in the heme degradation reaction by HutZ from *Vibrio cholerae*. *Dalton Trans.* **46,** 8104–8109 CrossRef Medline
36. Ulijasz, A. T., and Vierstra, R. D. (2011) Phytochrome structure and photochemistry: recent advances toward a complete molecular picture. *Curr. Opin. Plant Biol.* **14,** 498–506 CrossRef Medline
37. Peng, Y. J., Makarenko, V. V., Nanduri, J., Vasavda, C., Raghuraman, G., Yuan, G., Gadalla, M. M., Kumar, G. K., Snyder, S. H., and Prabhakar, N. R. (2014) Inherent variations in CO-H_2S-mediated carotid body O_2 sensing mediate hypertension and pulmonary edema. *Proc. Natl. Acad. Sci. U.S.A.* **111,** 1174–1179 CrossRef Medline
38. Peng, Y. J., Nanduri, J., Raghuraman, G., Souvannakitti, D., Gadalla, M. M., Kumar, G. K., Snyder, S. H., and Prabhakar, N. R. (2010) H_2S mediates O_2 sensing in the carotid body. *Proc. Natl. Acad. Sci. U.S.A.* **107,** 10719–10724 CrossRef Medline
39. Abe, K., and Kimura, H. (1996) The possible role of hydrogen sulfide as an endogenous neuromodulator. *J. Neurosci.* **16,** 1066–1071 CrossRef Medline
40. Taoka, S., and Banerjee, R. (2001) Characterization of NO binding to human cystathionine β-synthase: possible implications of the effects of CO and NO binding to the human enzyme. *J. Inorg. Biochem.* **87,** 245–251 CrossRef Medline
41. Yuan, G., Vasavda, C., Peng, Y. J., Makarenko, V. V., Raghuraman, G., Nanduri, J., Gadalla, M. M., Semenza, G. L., Kumar, G. K., Snyder, S. H., and Prabhakar, N. R. (2015) Protein kinase G-regulated production of H_2S governs oxygen sensing. *Sci. Signal.* **8,** ra37 CrossRef Medline
42. Peng, Y. J., Zhang, X., Gridina, A., Chupikova, I., McCormick, D. L., Thomas, R. J., Scammell, T. E., Kim, G., Vasavda, C., Nanduri, J., Kumar, G. K., Semenza, G. L., Snyder, S. H., and Prabhakar, N. R. (2017) Complementary roles of gasotransmitters CO and H_2S in sleep apnea. *Proc. Natl. Acad. Sci. U.S.A.* **114,** 1413–1418 CrossRef Medline
43. Hayashi, S., Takamiya, R., Yamaguchi, T., Matsumoto, K., Tojo, S. J., Tamatani, T., Kitajima, M., Makino, N., Ishimura, Y., and Suematsu, M. (1999) Induction of heme oxygenase-1 suppresses venular leukocyte adhesion elicited by oxidative stress: role of bilirubin generated by the enzyme. *Circ. Res.* **85,** 663–671 CrossRef Medline
44. Matera, K. M., Zhou, H., Migita, C. T., Hobert, S. E., Ishikawa, K., Katakura, K., Maeshima, H., Yoshida, T., and Ikeda-Saito, M. (1997) Histidine-132 does not stabilize a distal water ligand and is not an important residue for the enzyme activity in heme oxygenase-1. *Biochemistry* **36,** 4909–4915 CrossRef Medline
45. Fujii, H., Zhang, X., Tomita, T., Ikeda-Saito, M., and Yoshida, T. (2001) A role for highly conserved carboxylate, aspartate-140, in oxygen activation and heme degradation by heme oxygenase-1. *J. Am. Chem. Soc.* **123,** 6475–6484 CrossRef Medline
46. Sun, D., Sato, M., Yoshida, T., Shimizu, H., Miyatake, H., Adachi, S., Shiro, Y., and Kikuchi, A. (2000) Crystallization and preliminary X-ray diffraction analysis of a rat biliverdin reductase. *Acta Crystallogr. D Biol. Crystallogr.* **56,** 1180–1182 CrossRef Medline
47. Liu, Y., Moënne-Loccoz, P., Loehr, T. M., and Ortiz de Montellano, P. R. (1997) Heme oxygenase-1, intermediates in verdoheme formation and the requirement for reduction equivalents. *J. Biol. Chem.* **272,** 6909–6917 CrossRef Medline
48. Wilks, A., and Ortiz de Montellano, P. R. (1993) Rat liver heme oxygenase. High level expression of a truncated soluble form and nature of the *meso*-hydroxylating species. *J. Biol. Chem.* **268,** 22357–22362 Medline

Hydrogen sulfide bypasses the rate-limiting oxygen activation of heme oxygenase

Toshitaka Matsui, Ryota Sugiyama, Kenta Sakanashi, Yoko Tamura, Masaki Iida, Yukari Nambu, Tsunehiko Higuchi, Makoto Suematsu and Masao Ikeda-Saito

J. Biol. Chem. 2018, 293:16931-16939.
doi: 10.1074/jbc.RA118.004641 originally published online September 20, 2018